MULTISCALE METHODS FOR BOUNDARY INTEGRAL EQUATIONS AND THEIR APPLICATION TO BOUNDARY VALUE PROBLEMS IN SCATTERING THEORY AND GEODESY

Bernd H. Kleemann
Berliner Institut für Optik, GmbH
Rudower Chaussee 6
D–12484 Berlin, Germany

Andreas Rathsfeld
Weierstraß-Institut für
Angewandte Analysis und Stochastik
Mohrenstr. 39
D–10117 Berlin, Germany

Reinhold Schneider
Fachbereich Mathematik
Technische Hochschule Darmstadt
Schloßgartenstr. 7
D–64289 Darmstadt, Germany

SUMMARY

In the present paper we give an overview on multiscale algorithms for the solution of boundary integral equations which are based on the use of wavelets. These methods have been introduced first by Beylkin, Coifman, and Rokhlin [5]. They have been developed and thoroughly investigated in the work of Alpert [1], Dahmen, Proessdorf, Schneider [16-19], Harten, Yad-Shalom [25], v.Petersdorff, Schwab [33-35], and Rathsfeld [39-40]. We describe the wavelet algorithm and the theoretical results on its stability, convergence, and complexity. Moreover, we discuss the application of the method to the solution of a two-dimensional scattering problem of acoustic or electromagnetic waves and to the solution of a fixed geodetic boundary value problem for the gravity field of the earth. The computational tests confirm the high compression rates and the saving of computation time predicted by the theory.

Boundary element methods (BEM) are known to be a good tool for the solution of some classes of boundary value problems for partial differential equations. Frequently, however, the fact that the arising stiffness matrices are dense causes a lot of problems in the implementation. For example, the solution of a boundary element system with about 100 000 unknowns requires a storage capacity of about 80 Gigabytes. Clearly, also the computation time for the processing of such an amount of data is considerably long. To reduce storage and computation time, there have been introduced several methods. We only mention the method of multipole expansion by Rokhlin and Greengard [42,23], the panel clustering of Hackbusch and Nowak [24,46], and the splitting methods of Amosov [3], Saranen and Vainikko [44]. Note that *h-p* schemes can also be considered as a method to improve computation time and to reduce storage.

In the present paper, we will discuss algorithms which are called *multiscale methods* and which are well-known from their application to finite element methods. For finite element methods, however, the matrices of the linear equations are sparse, and the multiscale approach is used only to construct preconditioners for the iterative solution of the matrix equations. This feature is important for the BEMs, too. Namely, in case of integral operators of order different from zero, the condition numbers of the traditional BEM matrices increases rapidly if the mesh size tends to zero whereas the condition numbers of the BEM matrices corresponding to wavelet bases multiplied by diagonal preconditioners remain bounded. In addition to this preconditioning, the multiscale setting also provides a good tool to develop fast algorithms for the multiplication of a vector times the matrices of the BEM systems, i.e., to develop fast iterative solvers. This facility has been used without a wavelet frame by Brandt and Lubrecht [6] and together with a wavelet scheme in the pioneer paper by Beylkin, Coifman, and Rokhlin [5]. Note that throughout the present paper we will use the notion of wavelets in a generalized sense.

The *wavelet approach* has been thoroughly investigated and further developed by several authors. A new basis of multi wavelets for the discretization of integral equations has been introduced by Alpert [1] and a wavelet basis for the space of test functionals in case of collocation has been treated by Dahmen, Proessdorf, Schneider [16-19]., Harten, and Yad-Shalom [25]. Moreover, Dahmen, Proessdorf, and Schneider [16-19] were probably the first who have matched the compression error to the discretization error of the Galerkin and the collocation method, respectively. The same authors [19,47] have stressed the importance of higher orders for the dual wavelets in biorthogonal settings, and they have defined preconditioners for the BEM matrices corresponding to the wavelet basis [18] (cf. also [14,26,48]). A further improvement of the estimates for the error due to the compression as well as special aspects for special BEM applications have been investigated by v.Petersdorff and Schwab [34-35]. The final step in the reduction of the number of arithmetic operations has been achieved by Schneider [47]. He has proved that, for the computation of a numerical solution with N degrees of freedom approximating the exact solution with an error less than the usual discretization error, $O(N)$ matrix entries are sufficient. This result is obtained if the compression is extended to matrix entries corresponding to test and trial wavelets with overlapping support. Furthermore, a suitable quadrature algorithm for the computation of the stiffness matrix with respect to the wavelet bases has been developed simultaneously by Schneider [47], v.Petersdorff and Schwab [34] for the case of the Galerkin method and by Rathsfeld [39-40] for collocation.

The first results on wavelet methods over non-uniform grids are due to Rathsfeld [39], v. Petersdorff and Schwab [33]. The issue of adaptive wavelet methods has been discussed by Dahlke, Dahmen, Hochmuth, and Schneider [11]. Finally, we mention that the first steps to handle unstructured grids have been performed by Carnicer, Dahmen, Peña [7], and Sweldens [49] (cf. also [15]), and numerical tests have been reported e.g. in the papers by Dorobantu [21] and by Dahmen, Kleemann, Proessdorf, and Schneider [12,13].

The *plan of the paper* is as follows. In Section 2 we will make a few remarks on boundary integral operators and introduce the integral operators for the direct time-harmonic scattering problem and for the geodetic boundary value problem. The trial space and its multiscale decomposition will be introduced in Section 3. We will define the wavelet functions in a general setting. In particular, we will describe the piecewise linear wavelets with smallest support which are employed in the numerical experiments. Section 4 is devoted to the wavelet algorithm for the fast solution of the Galerkin BEM equations. Thus, we will present compression strategies, error estimates, a remark on the quadrature approximation, and theorems on the diagonal preconditioning. In Section 5 we will consider the collocation method in an analogous manner. We will introduce wavelet test functionals and define the wavelet algorithm for the collocation. Finally, we present the results of numerical tests.

2. BOUNDARY INTEGRAL OPERATORS

2.1. GENERAL BOUNDARY INTEGRAL OPERATORS

The first step of BEM consists in the reduction of boundary value problems to equivalent integral operators. For example, suppose a boundary value problem for an elliptic partial differential equation over a domain D in the $n+1$ dimensional Euclidean space $\mathbb{R}^{n+1}$ is to be solved. Then we can seek a solution in the form of an integral representation, e.g., in form of the representation formula for the solution of the partial differential equation. Clearly, the representation includes one or more yet unknown density functions defined over the boundary Γ of D. Applying the operator of the boundary value condition to this representation, we end up with one or more integral equations over Γ for the unknown density functions. With the BEM these integral equations are solved numerically. Finally, we get the solution to the boundary value problem by substituting the approximate density functions into the integral representation.

Now we suppose that the boundary Γ is piecewise smooth, i.e., we suppose Γ to be the union of the closed bounded surface pieces $\overline{\Gamma}_m$, $m = 1, \ldots, m_\Gamma$ such that, for every m, there exists a coordinate mapping $\kappa_m : \square \to \Gamma_m$ from a reference domain $\square \subseteq \mathbb{R}^n$ to Γ_m. The domain $\square$ is something like a unit square or a simple triangle, and the mapping κ_m is supposed to be continuously differentiable up to a certain degree. Moreover, we suppose that this mapping extends to a mapping over a small neighbourhood of $\square$. Note

that, frequently, the parametric surface representation is provided by CAD, CAGD (cf. e.g. freeform surfaces, NURBS, and the standards for format: IGES).

Usually, the boundary integral operator over Γ is a matrix of integral operators of different types. In the simplest case, the boundary integral equation takes the form

$$Au(x) \;:=\; au(x) + \int_\Gamma K_A(x,y)u(y)\mathrm{d}_y\Gamma \;=\; v(x), \quad x \in \Gamma, \tag{1}$$

where a is a constant and $K_A(x,y)$ is the so called Schwartz kernel of A. Frequently, the integral on the left-hand side of (1) is to be understood in a generalized sense. For a certain fixed $\mathbf{r}$, the kernel $K_A(x,y)$ satisfies the Calderon Zygmund estimate

$$|\partial_x^\alpha \partial_y^\beta K_A(x,y)| \le C(\alpha,\beta,A,\Gamma)\,|x-y|^{-(n+\mathbf{r}+|\alpha|+|\beta|)}\;, \tag{2}$$

provided $n+\mathbf{r}+|\alpha|+|\beta| > 0$. Note that $\mathbf{r}$ is called the order of A and that, for sufficiently smooth Γ and classical pseudodifferential operators A, the operator A maps the Sobolev space $H^s(\Gamma)$ into $H^{s-\mathbf{r}}(\Gamma)$. Usually, we have $a = 1,\ \mathbf{r} = 0$ or $a = 0,\ \mathbf{r} \neq 0$. Finally, we remark that, in local coordinates, (1) takes the form

$$\begin{aligned} Au(\kappa_k(t)) \;&=\; au(\kappa_k(t)) + \sum_{m=1}^{m_\Gamma} \int_\square K_A(\kappa_k(t),\kappa_m(s))u(\kappa_m(s))|\kappa_m'(s)|\mathrm{d}s \;=\; v(\kappa_k(t)), \\ &\qquad t \in \square,\ k = 1,\ldots,m_\Gamma, \end{aligned} \tag{3}$$

where $|\kappa_m'(s)|$ denotes the absolute value of the derivative $\kappa_m'(s)$ for $n = 1$ and the absolute value of the vector product $\partial_{s_1}\kappa_m(s) \times \partial_{s_2}\kappa_m(s)$ for $n = 2$.

For the stability of the numerical methods, the concept of strong ellipticity plays a crucial role. We call A strongly elliptic if A satisfies the so called Gårding inequality, i.e.,

$$\mathrm{Re}\langle Au, u\rangle_{L^2(\Gamma)} \ge \gamma\|u\|_{H^{r/2}(\Gamma)} - |\langle Tu, u\rangle_{L^2(\Gamma)}| \tag{4}$$

for any $u \in H^{\mathbf{r}/2}(\Gamma)$. In (4) the operator $T \in \mathcal{L}(H^{\mathbf{r}/2}(\Gamma), H^{-\mathbf{r}/2}(\Gamma))$ is supposed to be compact and γ stands for a positive constant independent of u.

2.2. AN INTEGRAL OPERATOR IN SCATTERING THEORY

Now we turn to a boundary integral equation for a scattering problem (for details cf. [10]). We consider the scattering of time–harmonic acoustic and electromagnetic waves by an infinitely long cylindrical obstacle with a simply connected bounded cross section $D_- \subset \mathbb{R}^2$. We suppose the boundary Γ of D_- to be analytic and set $D := \mathbb{R}^2 \setminus D_-$. The wave corresponding to a wave number $\bar{k}$ and defined in the outer domain D is the sum of a given incoming wave w^{in} and the unknown scattered wave w. For a sound-soft obstacle, this w is the solution of the following exterior boundary value problem for the Helmholtz equation:

$$\Delta w(x) + \bar{k}^2 w(x) \;=\; 0 \qquad \text{in} \quad D, \tag{5}$$

$$w(x) \;=\; -w^{\mathrm{in}}(x) \quad \text{on} \quad \Gamma\,, \tag{6}$$

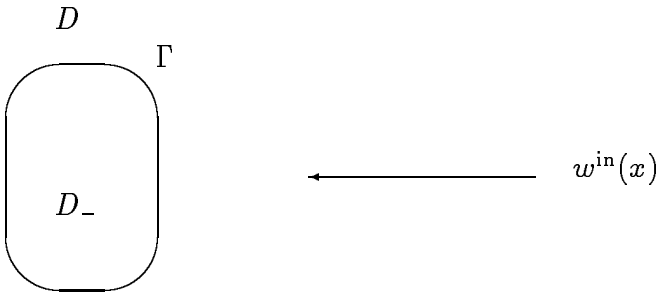

Figure 1: Scattering problem.

$$\frac{\partial w(x)}{\partial r} - \mathrm{i}\bar{k}w(x) \;=\; o(r^{-1/2})\,,\; r = |x| \to \infty\,. \tag{7}$$

Here (7) is supposed to hold uniformly in all directions. This condition is called Sommerfeld radiation condition. We seek w in form of a single-layer potential

$$w(x) = \frac{1}{2\mathrm{i}} \int_\Gamma H_0^{(1)}(\bar{k}|x-y|)\tilde{u}(y)\mathrm{d}_y\Gamma \tag{8}$$

with the Hankel function $H_0^{(1)}$ of order zero and of the first kind. Using the global parametrization $\kappa = (x_1, x_2) : \square \longrightarrow \Gamma$ over the 2π periodic interval $\square$, we arrive at the boundary integral equation

$$(Au)(t) := \frac{1}{2\pi} \int_0^{2\pi} K(t,\tau)u(\tau)\mathrm{d}\tau = v(t)\,,\; 0 \le t \le 2\pi, \tag{9}$$

where

$$\begin{aligned} u(t) &:= \tilde{u}(\kappa(t))\sqrt{[x_1'(t)]^2 + [x_2'(t)]^2}, \quad v(t) := -w^{\mathrm{in}}(\kappa(t))\,, \\ K(t,\tau) &:= \frac{\pi}{\mathrm{i}} H_0^{(1)}(\bar{k}r(t,\tau))\,,\; t \neq \tau\,, \\ r(t,\tau) &:= \sqrt{[x_1(t)-x_1(\tau)]^2 + [x_2(t)-x_2(\tau)]^2}\,. \end{aligned}$$

Note that the integral operator A on the left-hand side of (9) is strongly elliptic, its order $\mathbf{r}$ is -1, and the dimension of the boundary manifold is $n = 1$. In addition to (2), we have

$$|K(t,\tau)| \le C(0,0,A,\Gamma)\,\log\left(\max\{1, |t-\tau|^{-1}\}\right), \tag{10}$$

i.e., the integral equation has a logarithmic kernel.

Knowing the solution u of (9), several interesting quantities can be derived. The scattered wave w is known to have an asymptotics of the form

$$w(x) = \frac{\exp(\mathrm{i}\bar{k}|x|)}{\sqrt{|x|}} \left\{ u^\infty\left(\frac{x}{|x|}\right) + O\left(\frac{1}{|x|}\right)\right\}, \quad |x| \longrightarrow \infty. \tag{11}$$

Here, the function u^∞ is called the far field pattern or scattering amplitude of w. It can be expressed as a functional of the density $u = A^{-1}v$.

$$u^\infty\left(\frac{x}{|x|}\right) = \frac{\exp(\mathrm{i}\frac{\pi}{4})}{\sqrt{8\pi\bar{k}}}\int_0^{2\pi} u(t)\exp\left(-\mathrm{i}\bar{k}\frac{x}{|x|}\cdot\kappa(t)\right)\mathrm{d}t. \tag{12}$$

For $x/|x| = (\cos\theta, \sin\theta)$, the radar cross section is defined as the limit

$$\sigma^{\mathrm{c}}(\theta) := 2\pi \lim_{|x|\to\infty} x\frac{|w(x)|^2}{|w^{\mathrm{in}}(x)|^2}.$$

It is not hard to see that $\sigma^{\mathrm{c}}(\theta) = 2\pi|u^\infty(x/|x|)|^2$.

2.3. AN INTEGRAL OPERATOR IN GEODESY

One fundamental problem in geodesy consists in the computation of the gravity field around the earth from the gravity data measured over the known surface of the earth (for more details cf. [27,22]). In other words, if D is the exterior of the earth, Γ the earth's surface, ω the angular velocity of the rotation, g the gravity, and w the unknown potential of the gravity field, then w is the solution of

$$\begin{aligned} \Delta w(x) &= 2\omega^2, \quad x \in D, \\ |\mathrm{grad}\ w(x)| &= g(x), \quad x \in \Gamma. \end{aligned}$$

Introducing a well approximating reference potential $w_0 \approx w$ and neglecting higher order non-linear terms, we arrive at the following linear oblique derivative boundary value problem for the unknown difference potential $\delta w := w - w_0$:

$$\begin{aligned} \Delta[\delta w](x) &= 0, \qquad x \in D, \\ \partial_{l(x)}[\delta w](x) &= \delta g(x), \quad x \in \Gamma, \end{aligned}$$

where $\delta g := (g^2 - g_0^2)/2|g_0|$, $g_0 := \mathrm{grad}\ w_0$, and $l := g/|g_0|$. For the vector field l, we suppose that, at any $x \in \Gamma$, $l(x)$ is not tangential. We seek δw in form of a single layer potential with unknown density function $\tilde{u}$ over the earth's surface Γ.

$$\delta w(x) = \frac{1}{4\pi}\int_\Gamma \frac{\tilde{u}(y)}{|x-y|}\mathrm{d}_y\Gamma \tag{13}$$

Substituting this potential into the oblique derivative boundary condition and applying the jump relation for the gradient of the single layer potential, we obtain the following singular integral equation:

$$-2\pi\cdot\cos[\mathbf{n}(x), l(x)]\cdot\tilde{u}(x) + p.v.\int_\Gamma \frac{\cos[l(x), y-x]}{|y-x|^2}\cdot\tilde{u}(y)\cdot\mathrm{d}_y\Gamma \;=\; 4\pi\cdot\delta g(x). \tag{14}$$

Here $\mathbf{n}$ denotes the direction of the outward pointing normal on the earth's surface Γ and the integral is defined in the principal value sense (cf. [29]). Of course, we are not able to discretize the whole surface of the earth. This would require too much storage

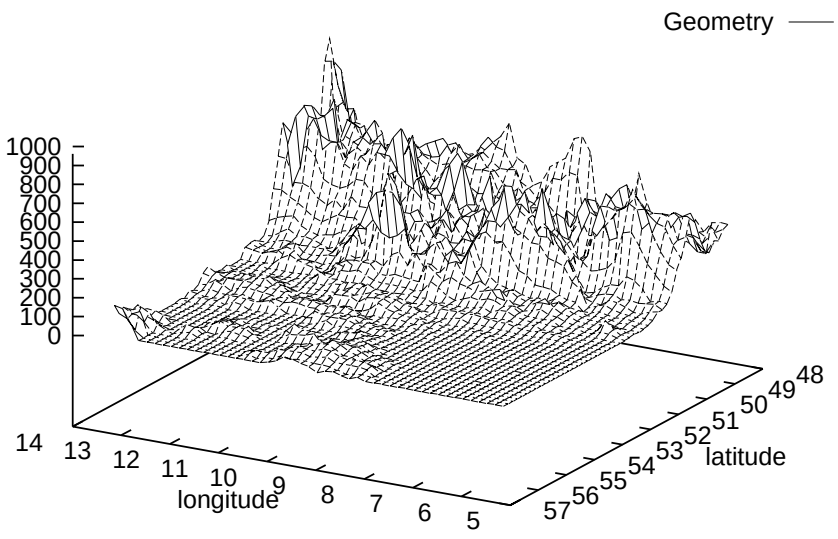

Figure 2: Height depending on latitude and longitude.

and computation time. Thus, we restrict the surface Γ to a quadratic surface piece of points with latitude between 48.60^0 and 56.65^0 and longitude between 5.35^0 and 13.40^0 (cf. Figure 2). Using a parametrization $\kappa : \square := [0,1] \times [0,1] \longrightarrow \Gamma$ based on Overhauser interpolation (cf. [32]) of uniformly distributed data, we transform (14) into the boundary integral equation $Au = v$ over $\square$ of the form

$$-2\pi \cos[\mathbf{n}(\kappa(t)), l(\kappa(t))]u(t) + p.v. \int_{\square} \frac{\cos[l(\kappa(t)), \kappa(s) - \kappa(t)]}{|\kappa(s) - \kappa(t)|^2} |\kappa(s)| u(s) \mathrm{d}s \;=\; v(t), \quad (15)$$

where $u(t) := \tilde{u}(\kappa(t))$ and $v(t) := 4\pi \cdot \delta g(\kappa(t))$. Note that the singular integral operator A is a strongly elliptic boundary integral operator defined over a "manifold" of dimension $n = 2$ and its order $\mathbf{r}$ is equal to zero.

3.1. THE WAVELET FUNCTIONS

The general theory of wavelets is exhibited in the text books [8,20,28]. In contrary to these books, we will immediately introduce wavelets on the manifold Γ. Thus, suppose that Γ is as in Section 2.1. Using the parametrizations, we can approximate boundary functions $u : \Gamma \to I\!R$ e.g. by curved finite elements. We chose a sequence of partitions over the reference domain $\square$ defined by the sets of grid points $\Delta_0 \subset \Delta_1 \subset \ldots \subset \Delta_j \subset \ldots$. The space of piecewise linear functions is spanned by the finite element basis $\{\varphi_k^{j,*} : k \in \Delta_j\}$ defined by $\varphi_k^{j,*}(k') = \delta_{k,k'},\ k' \in \Delta_j$. Analogously, the space of piecewise polynomials of degree less than d is spanned by similar basis functions over similar index sets. We suppose that these basis functions are normalized such that $\|\varphi_k^{j,*}\|_{L^2} \sim 1$. Setting $\varphi_{m,k}^j(x) = \varphi_k^{j,*}(\kappa_m^{-1}(x))\ ,\ x \in \Gamma_m$, we obtain the finite element space $\mathrm{span}\{\varphi_{m,k}^j : k \in \Delta_j\}$. We denote by S_j the intersection of the span of all these spaces defined for $m = 1, \ldots, m_\Gamma$ with the space $C^\sigma(\Gamma)$ of σ times continuously differentiable functions. In particular, we choose $\sigma = 0$ for the piecewise linear elements and $\sigma = -1$, i.e., no intersection with $C^\sigma(\Gamma)$, for the piecewise constant elements. We note here that a choice of higher values of σ can lead to a lot of difficulties, especially, for the subsequent constructions of wavelet bases. Even the case $\sigma = 0$ is not trivial. Nevertheless, we arrive at a multiscale analysis $S_0 \subset S_1 \subset \ldots \subset S_j \subset \ldots$ of order d ($d = 2$ for piecewise linear or bilinear functions and $d = 1$ for piecewise constants) and regularity $\gamma = \sigma + 3/2$. In other words, the spaces S_j are contained in the Soblolev spaces $H^s(\Gamma)$ of order s less than γ and the S_j contain polynomials of degree less than d. For these spaces S_j, we assume the approximation property

$$\inf_{u_j \in S_j} \|u - u_j\|_{H^s} \le C 2^{-j(t-s)} \|u\|_{H^t}, \qquad s \le t \le d,\ s < \gamma \tag{16}$$

and the inverse property

$$\|u_j\|_{H^t} \le C 2^{j(t-s)} \|u_j\|_{H^s}, \qquad s \le t < \gamma. \tag{17}$$

Now we set $W_{-1} = S_0$ and choose complement spaces W_j of the subspaces S_j in S_{j+1}. We arrive at the multiscale decomposition $S_j = \sum_{l=-1}^{j-1} W_l$ and call the elements of these complement spaces wavelets. By $\{\psi_{l,k}^m : m = 1, \ldots, m_\Gamma,\ k \in \nabla_l := \Delta_{l+1} \backslash \Delta_l\}$ we denote a basis of W_l which is supposed to satisfy $\|\psi_{l,k}^m \circ \kappa_m\|_{L^2} \sim 1$. The properties of the new basis and the basis transforms depend strongly on the dual multiscale decomposition. To introduce this, we define the duality pairing for functions over Γ by

$$\langle f, g \rangle := \sum_{m=1}^{m_\Gamma} \int_\square f(\kappa_m(s)) \overline{g(\kappa_m(s))} \mathrm{d}s, \tag{18}$$

and consider a dual multiscale analysis $\tilde{S}_0 \subset \tilde{S}_1 \subset \ldots \subset \tilde{S}_j \subset \ldots$ together with the dual multiscale decomposition $\tilde{S}_j = \sum_{l=-1}^{j-1} \tilde{W}_l$ and the basis functions $\tilde{\varphi}_{m,k}^j$ and $\tilde{\psi}_{l,k}^m$. Note that

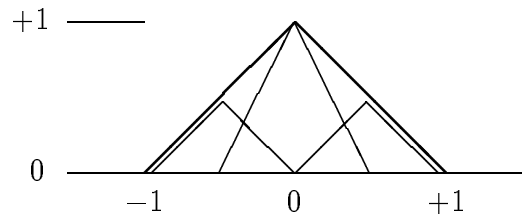

Figure 3: Scaling function φ and refinement equation.

the multiscale decomposition is called dual to $\{\psi_{l,k}^m\}$ if

$$\langle \varphi_{m,k}^j, \tilde{\varphi}_{m',k'}^j \rangle = \delta_{k,k'}\delta_{m,m'}, \quad \langle \psi_{l,k}^m, \tilde{\psi}_{l',k'}^{m'} \rangle = \delta_{l,l'}\delta_{k,k'}\delta_{m,m'}. \tag{19}$$

If such a dual system exists for $\{\psi_{l,k}^m\}$, then the wavelets $\psi_{l,k}^m$ are called biorthogonal wavelets (cf. [9]). We denote the order of the dual system by d^* and the parameter of regularity by γ^*.

For the wavelet algorithm applied to the BEM, the following two properties will be essential:

i) The wavelet functions $\psi_{l,k}^m$ are supposed to have a possibly small support. Typically, their support is the union of a small number of subdomains in the partition corresponding to the grid Δ_l.

ii) The wavelet functions $\psi_{l,k}^m$ with $l \geq 0$ fulfill the moment conditions of order d^*, i.e.,

$$\int_\square \psi_{l,k}^m(\kappa_m(s)) s^\alpha \mathrm{d}s \;=\; 0, \quad |\alpha| < d^*. \tag{20}$$

Clearly, condition ii) is a consequence of (19). If the properties i) and ii) are satisfied, then with the multiscale algorithm for the numerical solution of the boundary integral equation (1) over Γ we seek an approximate solution for the exact solution u in the form

$$u_j = \sum_{m=1}^{m_\Gamma} \sum_{l=-1}^{j-1} \sum_{k \in \nabla_l} u_{l,k}^m \psi_{l,k}^m. \tag{21}$$

Thus, the number N of degrees of freedom is of order $O(2^{jn})$. To simplify the subsequent formulae, we will assume $m_\Gamma = 1$ and we write $\kappa = \kappa_1$, $\varphi_k^j = \varphi_{1,k}^j$, and $\psi_{l,m} = \psi_{l,m}^1$. For the applications from Sections 2.2 and 2.3, the assumption $m_\Gamma = 1$ is satisfied.

3.2. PIECEWISE LINEAR AND BILINEAR WAVELETS

Now we consider the boundary curve Γ of Section 2.2 given via the global parametrization κ over $\square = [0, 2\pi]$. Since we solve the parameterized integral equation, we define the multiscale functions over the periodic interval $[0, 2\pi]$. This means we define the functions

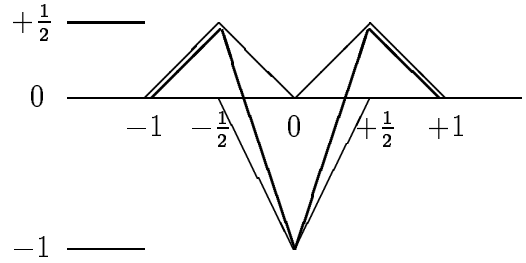

Figure 4: Mother wavelet ψ and two-scale relation.

as in the Section 3.1 but with Γ replaced by $[0,2\pi]$ and κ replaced by the identity mapping. For $[0,2\pi]$, the nested grids can be chosen as $\Delta^j := \{t_k^j : \ t_k^j := kh_j,\ k = 0,...,N-1\}$ with $h_j := 2^{-j} \cdot 2\pi$ and $N = N_j := 2^j$. The finite element basis function φ_k^j is given over $[t_{k-1}^j, t_{k+1}^j]$ by $\varphi_k^j(s) := \varphi(s/h_l - k)$ with

$$\varphi(s) \quad = \quad \begin{cases} 1-|s| & \text{if } \ |s|<1 \\ 0 & \text{else,} \end{cases} \tag{22}$$

(cf. Figure 3) and over $[0,2\pi] \setminus [t_{k-1}^j, t_{k+1}^j]$ we set φ_k^j to be zero. Note that the so called scaling function φ is a refinable function, i.e., we have (cf. Figure 3)

$$\varphi(x) = \frac{1}{2}\varphi(2x+1) + \varphi(2x) + \frac{1}{2}\varphi(2x-1). \tag{23}$$

In order to define the wavelet basis functions, we introduce the shape function ψ by (cf. Figure 4)

$$\psi(x) := \frac{1}{2}\varphi(2x+1) - \varphi(2x) + \frac{1}{2}\varphi(2x-1). \tag{24}$$

Note that ψ is called mother wavelet. Now the basis function $\psi_{l,k}$ on the grid of level l is the shift of the dilated function $\psi(\cdot/h_l)$ to the point t_k^{l+1} of the difference grid ∇_l, i.e., $\psi_{l,k}(t) := \psi((t - t_k^{l+1})/h_l)$ if $t \in [t_{k-2}^{l+1}, t_{k+2}^{l+1}]$ and $\psi_{l,k}(t) := 0$ else. It is not hard to see (cf. [39], Lemma 3.5) that these wavelets are biorthogonal in the sense of [9], with the exception that the dual wavelets have no finite support but decay exponentially. From [9] we infer that these functions represent a Riesz basis. Moreover, we get $d = 2,\ d^* = 2,\ \gamma = 3/2$.

Now we turn to the definition of bilinear wavelets for the boundary integral operator of Section 2.3. The boundary is given by the global parametrization κ over $\square = [0,1] \times [0,1]$. We define the functions as in Section 3.1 but with Γ replaced by $[0,1]\times[0,1]$ and κ replaced by the identity. Since the functions will be defined by tensor products, we begin with univariate functions over $[0,1]$. Analogously to the functions over the periodic interval $[0,2\pi]$, we introduce the one-dimensional grids Δ_j^B, ∇_l^B and the univariate functions $\varphi_k^{B,j}$ and $\psi_{l,k}^B$ over $[0,1]$. More exactly, we set $N_l := 3 \cdot 2^l$, $\Delta_l^B := \{k/N_l,\ k = 1,\ldots,N_l - 1\}$ and $\nabla_l^B := \Delta_{l+1} \setminus \Delta_l$ and take only the hat functions $\varphi_k^{B,j}(s) := \varphi(N_j s - k),\ k = 1,\ldots,N_j - 1$ vanishing at the end points of the interval. We define the wavelets $\psi_{l,k}^B$ analogously to the case of $[0,2\pi]$. However, we modify the $\psi_{l,k}^B$ for $k = 1$ and $k = N_{l+1} - 1$ such that they vanish at the end points, too. The two-dimensional wavelets are now the tensor products of these univariate functions. In other words, we set $\Delta_j := \Delta_j^B \times \Delta_j^B$ and $\nabla_l := \Delta_{l+1} \setminus \Delta_l = (\nabla_l^B \times \Delta_l^B) \cup (\Delta_l^B \times \nabla_l^B) \cup (\nabla_l^B \times \nabla_l^B)$ and define the bilinear multiscale

basis function by

$$\begin{aligned}
\psi_{-1,(k,m)}(s,t) &= \varphi_k^{B,0}(s)\cdot\varphi_m^{B,0}(t), \qquad (25)\\
\psi_{l,(k,m)}(s,t) &= \begin{cases} \psi_{l,k}^B(s)\cdot\varphi_m^{B,l}(t) & \text{if } k\in\nabla_l^B \text{ and } m\in\Delta_l^B \\ \varphi_k^{B,l}(s)\cdot\psi_{l,m}^B(t) & \text{if } m\in\nabla_l^B \text{ and } k\in\Delta_l^B \\ \psi_{l,k}^B(s)\cdot\psi_{l,m}^B(t) & \text{if } k,m\in\nabla_l^B, \end{cases} \qquad l=0,\ldots j-1.
\end{aligned}$$

For these wavelets, we again get $d=2,\ d^*=2$, and $\gamma=3/2$.

3.3. WAVELET TRANSFORMS AND GENERAL CONSTRUCTION OF WAVELETS

Now we return to the general case of Section 3.1. In the multiscale setting, we have the two basis $\{\varphi_k^j\}$ and $\{\psi_{l,k}\}$ of the trial space S_j. The corresponding basis transform T_j is called wavelet transform. More exactly, T_j is defined by $T_j(d_{l,k})_{l,k}=(c_k^j)_k$ if $\sum_{l=-1}^{j-1}\sum_{k\in\nabla_l} d_{l,k}\psi_{l,k}=\sum_{k\in\Delta_j} c_k^j\varphi_k^j$. These transforms T_j and their inverses are uniformly bounded with respect to the l^2 matrix norm if the wavelet functions represent a Riesz basis, i.e, if the L^2 norm of a function is equivalent to the l^2 norm of its coefficients with respect to the wavelet basis. For the biorthogonal bases of [9] and the representation $u_j=\sum_{l=-1}^{j-1}\sum_{k\in\nabla_l} d_{l,k}\psi_{l,k}$, we even have the more general norm equivalence valid for Sobolev spaces (cf. e.g. [31,14,47])

$$c_1\ \|u_j\|_{H^s}^2 \le \sum_{l=-1}^{j-1}\sum_{k\in\nabla_l} |2^{ls}d_{l,k}|^2 \le c_2\ \|u_j\|_{H^s}^2, \qquad (26)$$

where $\gamma^*<s<\gamma$ and c_1,c_2 denote non-negative constants. Note that this equivalence is fundamental for the preconditioning.

The application of the transform T_j can be realized by a fast pyramid scheme. To this end, we observe that the embeddings $S_j\subset S_{j+1}$ and $W_j\subset S_{j+1}$ imply the so called two-scale relations

$$\varphi_k^j = \sum_{q\in\Delta_{j+1}} m_{q,k}^{0,j}\varphi_q^{j+1},\quad k\in\Delta_j, \qquad (27)$$

$$\psi_{j,k} = \sum_{q\in\Delta_{j+1}} m_{q,k}^{1,j}\varphi_q^{j+1},\quad k\in\nabla_j:=\Delta_{j+1}\backslash\Delta_j. \qquad (28)$$

We introduce the corresponding matrices by $\mathbf{M}_{j,0}:=(m_{q,k}^{0,j})_{q\in\Delta_{j+1},k\in\Delta_j}$ and $\mathbf{M}_{j,1}:=(m_{q,k}^{1,j})_{q\in\Delta_{j+1},k\in\nabla_j}$. These matrices are sparse and, for the linear wavelets of Section 3.2, even band matrices since the two-scale relations (27) and (28) on arbitrary levels are similar two (23) and (24), respectively. Using the matrices $\mathbf{M}_{j,0}$ and $\mathbf{M}_{j,1}$, the transition from the representation $u^{j+1}=\sum_k c_k^j\varphi_k^j+\sum_k d_{j,k}\psi_{j,k}$ to the representation $u^{j+1}=\sum_k c_k^{j+1}\varphi_k^{j+1}$ is realized by the matrix multiplications $(c_k^{j+1})_k=\mathbf{M}_{j,0}(c_k^j)_k+\mathbf{M}_{j,1}(d_{j,k})_k$. Moreover, the transition from $u^j=\sum_{l=-1}^{j-1}\sum_k d_{l,k}\psi_{l,k}$ to $u^j=\sum_k c_k^j\varphi_k^j$ can be performed by stepping from level $l=0$ to level $l=j-1$ and multiplying by $\mathbf{M}_l:=(\mathbf{M}_{l,0},\mathbf{M}_{l,1})$ in each step. Indeed, if we set $d^l:=(d_{l,k})_k$ and $c^l:=(c_k^l)_k$ for $\sum_k c_k^l\varphi_k^l=\sum_{l'=-1}^{l-1}\sum_k d_{l',k}\psi_{l',k}$, then $c^j=T_j(d^l)_l$

can be computed by the multiplications corresponding to the pyramid scheme

$$\begin{array}{ccccccccccc} & d^0 & & & d^1 & & & \cdots & d^{j-1} & & \\ & & \searrow & & \mathbf{M}_{0,1} & \searrow & \mathbf{M}_{1,1} & & \searrow & & \mathbf{M}_{j-1,1} \\ d^{-1} & & \rightarrow & & c^1 & \rightarrow & c^2 & \cdots\ c^{j-1} & \rightarrow & & c^j \quad . \\ & & \mathbf{M}_{0,0} & & & \mathbf{M}_{1,0} & & & \mathbf{M}_{j-1,0} & & \end{array} \tag{29}$$

Since the matrices are sparse, the application of T_j requires only $O(N_j)$ operations, where N_j is the dimension of the space S_j.

For the inverse transform T_j^{-1}, we remark that, analogously to (27) and (28), we get the two-scale relation

$$\varphi_q^{j+1} = \sum_{k\in\Delta_j} g_{q,k}^{0,j}\varphi_k^j + \sum_{k\in\nabla_j} g_{q,k}^{1,j}\psi_{j,k},\ q\in\Delta_{j+1}. \tag{30}$$

We introduce the matrices $\mathbf{G}_{j,0} := (g_{q,k}^{0,j})_{q\in\Delta_{j+1},k\in\Delta_j}$, $\mathbf{G}_{j,1} := (g_{q,k}^{1,j})_{q\in\Delta_{j+1},k\in\nabla_j}$, $\mathbf{M}_j := (\mathbf{M}_{j,0},\mathbf{M}_{j,1})$ and $\mathbf{G}_j := (\mathbf{G}_{j,0},\mathbf{G}_{j,1})$. Clearly, $\mathbf{G}_j^* = \mathbf{M}_j^{-1}$ and the wavelet transform T_j^{-1} can be computed by running backward through (29). On each level we have to multiply by $\mathbf{G}_j^*$, which is a band matrix for the biorthogonal wavelets in [9]. In case of the linear wavelets of Section 3.2, $\mathbf{G}_j^*$ is not sparse anymore. However, the multiplication by $\mathbf{G}_j^*$ can be replaced by a fast solver for band matrices applied to the matrix equation including matrix $\mathbf{M}_j$.

Now we conclude this section with a remark on the construction of new wavelets. In many application, a simple wavelet basis with stable wavelet transforms T_j (i.e., the T_j and T_j^{-1} are uniformly bounded with respect to j) is available, however, these functions are not smooth enough or they do not satisfy the moment conditions of the desired order. Then the simple wavelets can be modified by changing the coefficients in the two-scale relations.

Lemma 1 [7,15,19,49] *Let* $\breve{\mathbf{M}}_j = (\mathbf{M}_{j,0},\breve{\mathbf{M}}_{j,1})$ *and* $\breve{\mathbf{G}}_j = (\breve{\mathbf{G}}_{j,0},\breve{\mathbf{G}}_{j,1}) = (\breve{\mathbf{M}}_j^{-1})^*$ *stand for the matrices of the simple and stable wavelets. Furthermore, suppose* $\mathbf{K}_j = (k_{q,k}^j)_{q,k\in\nabla_j}$ *is invertible and* $\mathbf{L}_j = (l_{q,k}^j)_{q\in\Delta_j,k\in\nabla_j}$ *is arbitrary. Then the matrix* $\mathbf{M}_{j,1} := \mathbf{M}_{j,0}\mathbf{L}_j + \breve{\mathbf{M}}_{j,1}\mathbf{K}_j$ *together with* $\mathbf{M}_{j,0}$ *defines another stable wavelet system, where* $\mathbf{G}_{j,0} := \breve{\mathbf{G}}_{j,0} - \breve{\mathbf{G}}_{j,1}(\mathbf{K}_j^*)^{-1}\mathbf{L}_j^*$, $\mathbf{G}_{j,1} := \breve{\mathbf{G}}_{j,1}(\mathbf{K}_j^*)^{-1}$.

In particular, one can choose $\mathbf{K}_j = \mathbf{I}$ to get $\psi_{j,k} = \sum_{q\in\Delta_j} l_{q,k}^j\varphi_q^j + \breve{\psi}_{j,k}$, $k\in\nabla_j$. Thus, for any given stable completion, it is possible to construct new wavelets with a desired order of vanishing moments. Note that a dual construction is also possible. Moreover, for sparse matrices $\breve{\mathbf{M}}_j$ and $\breve{\mathbf{G}}_j$ and suitable $\mathbf{K}_j$ and $\mathbf{L}_j$, the resulting matrices $\mathbf{M}_j$ and $\mathbf{G}_j$ are sparse again. As starting points for these constructions we can choose the discontinuous piecewise polynomials or hierarchical (nodal) basis functions for Lagrangian finite elements. Note that the values of the dual scaling functions can be obtained by the subdivision scheme

$$\begin{aligned} \lim_{J\to\infty}\sum_{\nu\in\Delta_J}\tilde{f}_{k,\nu}^{j,J}\varphi_\nu^J &= \tilde{\varphi}_k^j, \quad (\tilde{f}_{k,\nu}^{j,J})_{\nu\in\Delta_J} := \prod_{l=j}^{J}\mathbf{G}_{l,0}\mathbf{e}_k^j, \\ \mathbf{e}_k^j &:= (0,\cdots,\overset{k}{\breve{1}},\cdots,0)^{\mathrm{T}}. \end{aligned} \tag{31}$$

4.1. CONVENTIONAL GALERKIN SCHEMES

For the solution of the boundary integral equation (1), Galerkin schemes are very popular. With this scheme we seek an approximate solution $u_j \in S_j$ for the exact solution u of $Au = v$ by solving

$$\langle Au_j, w\rangle = \langle v, w\rangle, \quad w \in S_j. \tag{32}$$

These Galerkin equations are equivalent to the equation $Q_j^* A u_j = Q_j^* v$, where Q_j^* denotes the $\langle\cdot,\cdot\rangle$- adjoint operator of Q_j and Q_j stands for the orthogonal projection of $H^{\mathbf{r}/2}(\Gamma)$ onto S_j. Recall that $\mathbf{r}$ is the order of operator A. The Galerkin method is called stable in the Sobolev space H^s if, for sufficiently large j, the Galerkin operators $\mathcal{A}_j := Q_j^* A|_{S_j} \in \mathcal{L}(S_j)$ are invertible and the $(H^{s-\mathbf{r}}, H^s)$- norm of the inverse operators are uniformly bounded. The following result is well known:

Theorem 1 *If A is a bounded, strongly elliptic, and invertible operator mapping H^s into $H^{s-\mathbf{r}}$ for $\mathbf{r} - d \le s \le d$, then the Galerkin method is stable in H^s for $\mathbf{r} - \gamma < s < \gamma$. The approximate solution u_j of (32) converges in H^s to the exact solution u of $Au = v$ for any $v \in H^{s-\mathbf{r}}$ with $s > \mathbf{r} - \gamma$ and the Galerkin error $\|u - u_j\|_{H^s}$ is less than $C2^{-j(t-s)}\|u\|_{H^t}$ for $\mathbf{r} - d \le s \le t \le d,\ s < \gamma,\ \mathbf{r} - \gamma < t$.*

The conventional BEM algorithm determines the Galerkin solution u_j with respect to the finite element basis. In view of (32), the coefficients u_k^j of $u_j = \sum_{k\in\Delta_j} u_k^j \varphi_k^j$ are obtained by solving the linear system

$$\sum_{k\in\Delta_j} \langle A\varphi_k^j, \varphi_{k'}^j\rangle u_k^j = \langle v, \varphi_{k'}^j\rangle \quad , \quad k' \in \Delta_j \ . \tag{33}$$

The condition number $\|A_j\|_{\mathcal{L}(l^2)} \cdot \|A_j^{-1}\|_{\mathcal{L}(l^2)}$ of the $N \times N$ matrix $A_j := (\langle A\varphi_k^j, \varphi_{k'}^j\rangle)_{k',k\in\Delta_j}$ is of order $O(2^{j|\mathbf{r}|})$. Thus, to find efficient iterative algorithms for (33) with $\mathbf{r} \neq 0$ is a difficult task. Diagonal preconditioners are not suitable.

4.2. THE WAVELET ALGORITHM

The wavelet method determines the Galerkin solution u_j in form of the wavelet representation $u_j = \sum_l \sum_k u_{l,k}\psi_{l,k}$. The unknown coefficients $u_{l,k}$ are the solutions of the system

$$\sum_{l=-1}^{j-1} \sum_{k\in\nabla_l} \langle A\psi_{l,k}, \psi_{l',k'}\rangle u_{l,k} = \langle v, \psi_{l',k'}\rangle, \quad k' \in \nabla_{l'}, \quad -1 \le l' \le j-1 \ . \tag{34}$$

For the preconditioning of the corresponding matrix $\tilde{A}_j := (\langle A\psi_{l,k}, \psi_{l',k'}\rangle)_{(l',k'),(l,k)}$, we introduce the diagonal matrix $D_j^\sigma := (2^{\sigma l}\delta_{l,l'}\delta_{k,k'})_{(l',k'),(l,k)}$.

Theorem 2 [18,14,47] *Suppose $\gamma^* > -\frac{\mathbf{r}}{2}$. The condition numbers of the preconditioned matrices $D_j^{-\mathbf{r}/2}\tilde{A}_j D_j^{-\mathbf{r}/2}$ are uniformly bounded with respect to j.*

Consequently, the system (34) can be solved iteratively with a number of iterations not depending on the mesh size 2^{-j}.

Another advantage of the wavelet basis consists in the pseudo locality of the operator representation, i.e., if the supports of the trial basis function $\psi_{l,k}$ and the test wavelet $\psi_{l',k'}$ are far from each other, then the corresponding matrix entry is small. Even if the support of one of these two wavelets is contained in the support of the other wavelet and if the distance of the first support to the discontinuity points of the other wavelet is relatively large, then the entry is small again.

Lemma 2 *a)* [5,18,35,47] *If $n + 2d^* + \mathbf{r} > 0$ and if $\operatorname{dist}(\operatorname{supp}\psi_{l,k}, \operatorname{supp}\psi_{l',k'}) > 0$ then, for the corresponding entry of $\tilde{A}_j$, we get*

$$|\langle A\psi_{l,k}, \psi_{l',k'}\rangle| \le C\, \frac{2^{l(-\frac{n}{2}-d^*)}2^{l'(-\frac{n}{2}-d^*)}}{[\operatorname{dist}(\operatorname{supp}\psi_{l,k}, \operatorname{supp}\psi_{l',k'})]^{n+\mathbf{r}+2d^*}}. \tag{35}$$

b) [47] *If $\operatorname{supp}\psi_{l,k}$ is contained in $\operatorname{supp}\psi_{l',k'}$ such that $\operatorname{supp}\psi_{l,k}$ does not intersect the set $\operatorname{sing\,supp}\psi_{l',k'}$ of discontinuity points for $\psi_{l',k'}$ and the derivatives of $\psi_{l',k'}$, then we get*

$$|\langle A\psi_{l,k}, \psi_{l',k'}\rangle| \le C\, \frac{2^{l(-\frac{n}{2}-d^*)}2^{l'(-\frac{n}{2})}}{[\operatorname{dist}(\operatorname{supp}\psi_{l,k}, \operatorname{sing\,supp}\psi_{l',k'})]^{n+\mathbf{r}+d^*}}. \tag{36}$$

A similar estimate holds if the roles of $\psi_{l,k}$ and $\psi_{l',k'}$ are interchanged.

Knowing these decay properties, we can set up a compressed matrix such that the additional error due to the neglect of small matrix entries is less than the discretization error in Theorem 1. We choose constants $a_i > 0,\ i = 0,\dots,3,\ \alpha \ge 0,\ \beta_i,\ i = 1,\dots,6$ and set

$$\begin{aligned} \mathcal{B}_{l,l'} &:= \max\{a_0 2^{-l}, a_0 2^{-l'}, a_1 j^\alpha 2^{\beta_1 j - \beta_2 l - \beta_3 l'}\}, \\ \mathcal{B}^S_{l,l'} &:= \max\{a_2 2^{-\max\{l,l'\}}, a_3 2^{\beta_4 j - \beta_5 \max\{l,l'\} - \beta_6(l+l')}\}. \end{aligned} \tag{37}$$

With these constants, the compressed matrix $A_j^\varepsilon = (a^\varepsilon_{(l',k'),(l,k)})_{(l',k'),(l,k)}$ is defined by

$$a^\varepsilon_{(l',k'),(l,k)} := \begin{cases} \langle A\psi_{l,k}, \psi_{l',k'}\rangle\ , & \text{if } \operatorname{dist}(\operatorname{supp}\psi_{l,k}, \operatorname{supp}\psi_{l',k'}) \le \mathcal{B}_{l,l'} \\ & \text{and if} \\ & \quad \text{either } \operatorname{dist}(\operatorname{supp}\psi_{l,k}, \operatorname{sing\,supp}\psi_{l',k'}) \le \mathcal{B}^S_{l,l'} \\ & \qquad \text{for } l \ge l' \\ & \quad \text{or } \operatorname{dist}(\operatorname{supp}\psi_{l',k'}, \operatorname{sing\,supp}\psi_{l,k}) \le \mathcal{B}^S_{l,l'} \\ & \qquad \text{for } l' \ge l \\ 0\ , & \text{otherwise.} \end{cases} \tag{38}$$

By $\mathcal{A}_j^\varepsilon \in \mathcal{L}(S_j)$ we denote the operator whose matrix $(\langle \mathcal{A}_j^\varepsilon \psi_{l,k}, \psi_{l',k'}\rangle)_{(l',k'),(l,k)}$ is A_j^ε. Further, we denote by $u_j^\varepsilon = \sum_l \sum_k u^\varepsilon_{l,k}\psi_{l,k}$ the solution of $\mathcal{A}_j^\varepsilon u_j^\varepsilon = Q_j^* v$, i.e., of

$$\sum_{l=-1}^{j-1}\sum_{k\in\nabla_j} a^\varepsilon_{(l',k'),(l,k)} u^\varepsilon_{k,l} = \langle v, \psi_{k',l'}\rangle, \quad l' = -1,\dots,j-1,\ k' \in \nabla_{l'}. \tag{39}$$

Theorem 3 *Suppose that the assumptions of Theorem 1 are satisfied and that* $d^* > d - \mathbf{r}$. *Moreover, with* $d' \in (d, d^* + \mathbf{r})$ *we choose* $\alpha = 0$, $\beta_1 = \beta_4 = (2d' - \mathbf{r})/(2d^* + \mathbf{r})$, $\beta_2 = \beta_3 = (d' + d^*)/(2d^* + \mathbf{r})$, $\beta_5 = d^*/(2d^* + \mathbf{r})$, *and* $\beta_6 = d'/(2d^* + \mathbf{r})$. *If the constants* a_i, $i = 0, \ldots, 3$ *are sufficiently large and if* A_j^ε *is given by (38), then:*

i) The sequence $\{\mathcal{A}_j^\varepsilon\}$ *is stable in* H^s *for* $\mathbf{r} - \gamma < s < \gamma$.

ii) The number of non-zero entries in A_j^ε *is less than* $O(N) = O(2^{nj})$.

iii) The error $\|u - u_j^\varepsilon\|_{H^s}$ *is bounded by* $O(2^{-j(t-s)}\|u\|_{H^t})$ *for* $\mathbf{r} - d \le s \le t \le d$, $s < \gamma$, $\mathbf{r}/2 \le t$.

4.3. THE ASSEMBLING OF THE MATRIX VIA QUADRATURE ALGORITHM

Normally, the major part of the computation time for the BEM is spent for the assembling of the stiffness matrix. The subsequent solution of the matrix equation is much faster. This ratio of computation times does not change even for the wavelet method. In view of the fact that we have to compute a compressed sparse matrix instead of the full matrix (cf. Theorem 3 ii)), we expect the same reduction of the computation time for the assembling of the matrix as for the iterative solution of the linear system. If analytic formulae for the computation of the matrix entries are available, then the development of an efficient algorithm for the matrix assembling should be easy. However, if the entries are to be computed by quadrature, then it is not so easy to set up a quadrature algorithm such that the numerical error due to the quadrature does not exceed the discretization error (cf. the Galerkin error in Theorem 1) and that the number of quadrature knots is essentially less than that for the conventional BEM. At least for piecewise analytic boundaries Γ and piecewise analytic kernel functions $K_A(x, y)$, the compressed matrix can be computed by quadrature with no more than $O(N)$ times a power of $\log N$ operations. The corresponding quadrature algorithms are due to v.Petersdorff, Schwab [34], and Schneider [47] (cf. also [15]). We will mention four fundamental principles of the algorithm, only. Note that, for the matrix entry $\langle A\psi_{l,k}, \psi_{l',k'}\rangle$, we have to compute

$$\int_{\tau'}\int_{\tau} \psi_{l',k'}(\kappa(x))K_A(\kappa(x),\kappa(y))\psi_{l,k}(\kappa(y))|\kappa'(y)|\,|\kappa'(x)|\mathrm{d}y\mathrm{d}x, \tag{40}$$

where $\tau \subset \operatorname{supp}\psi_{l,k}$ and $\tau' \subset \operatorname{supp}\psi_{l',k'}$ denote closed patches of the partitions on level l and l', respectively. The wavelets $\psi_{l,k} \circ \kappa$ and $\psi_{l',k'} \circ \kappa$ restricted to τ and τ', respectively, are polynomials of degree less than d. The quadrature algorithm for the assembling of the stiffness matrix A_j^ε should be based on the following:

i) If the order $\mathbf{r}$ of A is non-negative, then the integrals in (40) for $\tau \cap \tau' \neq \emptyset$ are singular or hypersingular. These integrals should be regularized before quadrature rules are applied (cf. [30,45,34]).

ii) For $\tau = \tau'$ as well as for τ and τ' sharing a common edge or vertex, the integrals in (40) are to be treated by transformation techniques (cf. [45,34]).

iii) If $\tau \cap \tau' = \emptyset$, then the domains τ and τ' should be divided in a further step. The final quadrature partitions $\tau = \cup_i \tau_i$ and $\tau' = \cup_m \tau'_m$ should satisfy

$$\operatorname{dist}(\tau'_m, \tau_i) \geq Q \max\{\operatorname{diam} \tau'_m, \operatorname{diam} \tau_j\}, \tag{41}$$

where Q is a fixed positive constant.

iv) The integrals of (40) restricted to $\tau'_m \times \tau_i$ should be approximated by tensor product Gauß rules. The orders of the Gauß rules should be chosen using quadrature estimates for analytic functions. Following this idea, the Gauß orders increase logarithmically with decreasing distance $\operatorname{dist}(\tau'_m, \tau_i)$.

5. THE COLLOCATION METHOD

5.1. THE CONVENTIONAL COLLOCATION

Suppose we seek an approximate solution $u_j \in S_j$ for the solution of the boundary integral equation $Au = v$. If u_j is determined by the Galerkin equation (32) or (34), then we have to compute stiffness matrices the entries of which contain double integrals (cf. (40)). In order to reduce the amount of work for the quadrature, the Galerkin equations are replaced by the simpler collocation equations. For this, we suppose that S_j is the space of piecewise linear or n- linear continuous functions defined over the partition on the j-th level, i.e., S_j is of order $d = 2$ and γ is equal to $3/2$. The collocation solution $u_j \in S_j$ is the solution of

$$(Au_j)(\kappa(k)) = v(\kappa(k)), \quad k \in \Delta_j. \tag{42}$$

Recall that Δ_j is the set of grid points of the level j partition on which S_j is defined. We introduce the interpolation projection P_j onto S_j by

$$P_j f \in S_j, \quad P_j f(\kappa(k)) = f(\kappa(k)), \quad k \in \Delta_j. \tag{43}$$

Clearly, the collocation system (42) is equivalent to $P_j A u_j = P_j v$. Analogously to the Galerkin method, the collocation is called stable in H^s if, for sufficiently large j, the collocation operators $\mathcal{A}_j := P_j A|_{S_j} \in \mathcal{L}(S_j)$ are invertible and the $(H^{s-\mathbf{r}}, H^s)$- norms of the inverse operators are uniformly bounded.

Theorem 4 *i)* [36,4,38] *Suppose that Γ is at least three times continuously differentiable and homeomorphic to the n-dimensional torus and that $\kappa : \square = [0,1]^n \longrightarrow \Gamma$ is a global parametrization. We assume that S_j is the set of n- linear splines defined over the uniform partition of $\square$ into 2^{nj} n-cubes (cf. Section 3). Moreover, we assume A to be a strongly*

elliptic classical pseudo-differential operator of order $\mathbf{r} < 1$. *Then the collocation method is stable in* H^s *for* $\mathbf{r} \le s < \frac{3}{2}$. *The collocation solution* u_j *defined by (42) converges in* H^s *to the exact solution* u *of* $Au = v$ *for any* $v \in H^{s-\mathbf{r}}$ *with* $s > \mathbf{r} + \frac{1}{2}$, *and the collocation error* $\|u_j - u\|_{H^s}$ *is bounded by* $C2^{-j(t-s)}\|u\|_{H^t}$ *for* $\mathbf{r} \le s \le t \le 2$, $s < \frac{3}{2}$, $\mathbf{r} + \frac{n}{2} < t$.
ii) [37] *Suppose that* $\Gamma = [0,1] \times [0,1]$, *that* S_j *and* Δ_j *are defined over* Γ *as in Section 3.2, and that* A *is a strongly elliptic pseudo-differential operator of order* $\mathbf{r} = 0$. *Then the collocation method is stable in* L^2. *The collocation solution* u_j *defined by (42) converges in* L^2 *to the exact solution* u *of* $Au = v$ *for any* $v \in L^2$ *such that* $\|P_j v - v\|_{L^2} \longrightarrow 0$. *If* u *is in* H^2 *and vanishes over the boundary of* $[0,1] \times [0,1]$, *then* $\|u_j - u\|_{L^2}$ *is less than* $C2^{-2j}\|u\|_{H^2}$.

Choosing the conventional finite element basis $\{\varphi_k^j\}_{k \in \Delta_j}$, the collocation equation (42) is equivalent to the system

$$\sum_{k \in \Delta_j} (A\varphi_k^j)(\kappa(k'))u_k^j = f(\kappa(k')), \quad k' \in \Delta_j \tag{44}$$

for the coefficients u_k^j of $u_j := \sum_{k \in \Delta_j} u_k^j \varphi_k^j$. Thus, the stiffness matrix of the collocation is $A_j := ((A\varphi_k^j)(\kappa(k')))_{k',k \in \Delta_j}$. The condition number of A_j is of order $O(2^{j|\mathbf{r}|})$ and, for $\mathbf{r} \neq 0$, the construction of efficient preconditioners is difficult.

5.2. WAVELETS IN THE SPACE OF TEST FUNCTIONALS

The space of test functionals in case of the collocation method (42) is spanned by the Dirac delta functionals $\{\delta_{\kappa(k)},\ k \in \Delta_j\}$, i.e., by the functionals of function evaluation at the collocation points. Following Brandt, Lubrecht [6], Harten and Yad-Shalom [25], we can introduce a basis of wavelet functionals in this space. For simplicity, we take wavelets with one or two vanishing moments and restrict the consideration first to the case that $\Gamma = \square$ is the periodic interval $[0, 2\pi]$ and later to $\square = [0,1] \times [0,1]$. In other words, we define the wavelets for the test functionals employed in the numerical tests for the solution of the boundary integral equations from Sections 2.2 and 2.3.

For $\Gamma = \square = [0, 2\pi]$, we retain the notation of Section 3.2 and introduce the wavelet functionals

$$\begin{aligned} \eta_{-1,k}(f) &:= f(t_k^0), && k \in \Delta_0, \\ \eta_{l,k}(f) &:= f(t_k^{l+1}) - \frac{1}{2}\{f(t_{k-1}^{l+1}) + f(t_{k+1}^{l+1})\}, && k \in \nabla_l, l = 0, \ldots, j-1. \end{aligned} \tag{45}$$

It is not hard to verify that the basis functionals $\eta_{l,k}$ span the space $\mathrm{span}\{\delta_{\kappa(k)},\ k \in \Delta_j\}$. They satisfy the second order moment conditions, i.e., they vanish at constant and linear functions. Furthermore, it is easy to see that the "classical" hierarchical basis $\{\varphi_k^{l+1},\ l = -1, \ldots, j-1,\ k \in \nabla_l\}$ is dual to $\{\eta_{l,k}\}$, i.e., $\eta_{l,k}(\varphi_{k'}^{l'+1}) = \delta_{l,l'}\delta_{k,k'}$ for $l, l' = -1, \ldots, j-1$ and $k \in \nabla_l,\ k' \in \nabla_{l'}$. Consequently, the interpolation $P_j f$ can be written as $\sum_l \sum_k \eta_{l,k}(f)\, \varphi_k^{l+1}$ and, analogously to (26), we arrive at

$$c_1\ \|u_j\|_{H^s}^2 \le \sum_{l=-1}^{j-1} \sum_{k \in \nabla_l} |2^{ls}\eta_{l,k}(u_j)|^2 \le c_2\ \|u_j\|_{H^s}^2, \tag{46}$$

where $\frac{1}{2} < s < \frac{3}{2}$. Now, the wavelet transform with respect to the dual basis maps the vector $(f(t_k^j))_{k\in\Delta_j}$ into the vector $(\eta_{l,k}(f))_{l=-1,\dots,j-1,\ k\in\nabla_l}$, and the inverse transform vice versa. If $(f(t_k^j))_{k\in\Delta_j}$ is known, than $(\eta_{l,k}(f))_{l=-1,\dots,j-1,\ k\in\nabla_l}$ can be computed directly by (45). For the inverse transform, a pyramid scheme should be applied. The transition from level l to level $l+1$ is accomplished by using the two-scale relation (45). Note that, for $t_k^{l+1} \in \nabla_l \subset \Delta_{l+1}$ the neighbours $t_{k\pm1}^{l+1}$ belong to Δ_l.

Now consider $\Gamma = \square = [0,1]\times[0,1]$. Retaining the definitions of $\Delta_l := \Delta_l^B \times \Delta_l^B$ and $\nabla_l = \Delta_{l+1} \setminus \Delta_l$ from Section 3.2, we define the test wavelets

$$\begin{aligned}
\eta_{-1,(k,m)}(f) &= f\left(\frac{k}{N_0},\frac{m}{N_0}\right), \qquad (47)\\
\eta_{l,(k,m)}(f) &= \begin{cases} f\left(\frac{k}{N_{l+1}},\frac{m}{N_{l+1}}\right) - f\left(\frac{k+1}{N_{l+1}},\frac{m}{N_{l+1}}\right) & \text{if } k\in\nabla_l^B \text{ and } m\in\Delta_l^B\\ f\left(\frac{k}{N_{l+1}},\frac{m}{N_{l+1}}\right) - f\left(\frac{k}{N_{l+1}},\frac{m+1}{N_{l+1}}\right) & \text{if } m\in\nabla_l^B \text{ and } k\in\Delta_l^B\\ f\left(\frac{k}{N_{l+1}},\frac{m}{N_{l+1}}\right) - f\left(\frac{k}{N_{l+1}},\frac{m+1}{N_{l+1}}\right) & \text{if } k,m\in\nabla_l^B,\end{cases}\\
&\qquad\qquad l = 0,\dots j-1.
\end{aligned}$$

It is not hard to verify that the basis functionals $\eta_{l,k},\ l=-1,\dots,j-1,\ k\in\nabla_l$ span the space $\mathrm{span}\{\delta_{\kappa(k)},\ k\in\Delta_j\}$. They satisfy the first order moment condition, i.e., they vanish at constant functions. The dual basis is a hierarchical basis of piecewise constant functions, and the wavelet transforms can be computed like those for the univariate case. Unfortunately, there is no analogue to (46).

5.3. THE WAVELET COLLOCATION METHOD

The wavelet method determines the solution u_j in form of the wavelet representation $u_j = \sum_{l=-1}^{j-1}\sum_{k\in\nabla_l} u_{l,k}\psi_{l,k}$. The unknown coefficients $u_{l,k}$ are the solutions of the system

$$\sum_{l=-1}^{j-1}\sum_{k\in\nabla_l} \eta_{l',k'}(A\psi_{l,k})\,u_{l,k} = \eta_{l',k'}(v), \qquad k'\in\nabla_{l'},\quad -1\le l'\le j-1\ . \qquad (48)$$

For the preconditioning of the corresponding stiffness matrix $\tilde{A}_j := (\eta_{l',k'}(A\psi_{l,k}))_{(l',k'),(l,k)}$, we recall the definition $D_j^\sigma := (2^{\sigma l}\delta_{l,l'}\delta_{k,k'})_{(l',k'),(l,k)}$.

Theorem 5 [47] *Suppose $n=1$ and that the assumptions of Theorem 4 i) are satisfied. Then, for $\frac{1}{2} < t < \frac{3}{2}$, the condition numbers of the matrices $D_j^{-\mathbf{r}+t}\tilde{A}_j D_j^{-t}$ are uniformly bounded with respect to j.*

Consequently, the system (48) can be solved iteratively with a number of iterations not depending on the mesh size 2^{-j}. For example, we consider the preconditioning for the boundary integral operator of Section 2.2, where the original cross section is an ellipse. Observing $\mathbf{r} = -1$, we arrive at the preconditioned matrices $D_j^{1+t}\tilde{A}_j D_j^{-t}$. However, taking the dependences on the wave number $\bar{k}$ into account, the preconditioner could be slightly improved. We replace D_j^t by $D_{\bar{k},j}^t := (\{\bar{k}^2 + 2^{2l}\}^{t/2}\delta_{l,l'}\delta_{k,k'})_{(l',k'),(l,k)}$. In Table 1 we present the numbers of GMRes iterations (cf. [43,50]) and the computation times for several types of preconditioning applied to the compressed stiffness matrix (cf. the subsequent

Preconditioning												
j	2	3	4	5	6	7	8	9	10	11	12	12
N_j	4	8	16	32	64	128	256	512	1024	2048	4096	4096
without	3	5	9	14	18	21	29	33	37	40	44	160.3s
$D_j^1 A_j^\varepsilon$	3	5	9	15	18	20	25	27	28	28	29	104.6s
$D_j^{\frac{1}{2}} A_j^\varepsilon D_j^{\frac{1}{2}}$	3	5	9	15	17	19	24	27	26	26	27	96.4s
$A_j^\varepsilon D_{k,j}^1$	3	5	9	14	**15**	**16**	**21**	**23**	**23**	**22**	**22**	81.5s

Table 1: Number of GMRes iterations and computation time for the iterative solver.

Theorem 6). The computations have been performed on a DEC 3000 AXP 600 α-processor workstation for the case of an ellipse Γ and a wave number $\bar{k} = 10$. The results show that the number of iterations are independent of the mesh size and that they are essentially reduced by the preconditioning.

Now it is not hard to see that a lemma analogously to Lemma 2 is valid for the collocation, too. Hence, we can set up a compressed matrix $A_j^\varepsilon = (a^\varepsilon_{(l',k'),(l,k)})_{(l',k'),(l,k)}$ by (cf. (37))

$$a^\varepsilon_{(l',k'),(l,k)} := \begin{cases} \eta_{l',k'}(A\psi_{l,k}) & \text{if } \operatorname{dist}(\operatorname{supp}\psi_{(l,k)}, \operatorname{supp}\eta_{(l',k')}) \le \mathcal{B}_{l,l'} \\ 0\ , & \text{otherwise.} \end{cases} \tag{49}$$

Introducing the dual basis $\{\tilde{\psi}_{l,k}\}_{l,k}$ of $\{\eta_{l,k}\}_{l,k}$, we define by $\mathcal{A}_j^\varepsilon$ the operator mapping S_j into $\operatorname{span}\{\tilde{\psi}_{l,k}\}_{l,k}$ whose matrix with respect to the bases $\{\psi_{l,k}\}_{l,k}$ and $\{\tilde{\psi}_{l,k}\}_{l,k}$ is A_j^ε. Further, we denote by $u_j^\varepsilon = \sum_l \sum_k u^\varepsilon_{l,k}\psi_{l,k}$ the solution of

$$\sum_{l=-1}^{j-1} \sum_{k\in\nabla_l} a^\varepsilon_{(l',k'),(l,k)} u^\varepsilon_{l,k} = \eta_{k',l'}(v), \quad l' = -1,\dots,j-1,\ k' \in \nabla_{l'}, \tag{50}$$

and let $\tilde{d}^*$ stand for the number of vanishing moments of the test wavelets $\eta_{l,k}$, $l \ge 0$. We have $\tilde{d}^* = 2$ for the univariate wavelets of Section 5.2 and $\tilde{d}^* = 1$ for the two-dimensional wavelets.

Theorem 6 [17,18,47] *Suppose that the assumptions of Theorem 4 i) or ii) are satisfied and that the number d^* of vanishing moments for the trial wavelets is greater than $-\mathbf{r}$. Choosing $d' \in (d, \tilde{d}^* + \mathbf{r})$, we set $\alpha = 5/[2(2+\mathbf{r}+\tilde{d}^*)]$, $\beta_1 = (d'-\mathbf{r})/(2+\mathbf{r}+\tilde{d}^*)$, $\beta_2 = \tilde{d}^*/(2+\mathbf{r}+\tilde{d}^*)$, and $\beta_3 = (d'+2)/(2+\tilde{d}^*)$. If the a_i, $i = 0,1$ are sufficiently large and if $\mathcal{A}_j^\varepsilon$ is given by (49), then:*

i) The sequence $\{\mathcal{A}_j^\varepsilon\}$ is stable in H^s for $\mathbf{r} \le s < \frac{3}{2}$.

ii) The number of non-zero entries in A_j^ε is less than $O(N \log N) = O(j2^{nj})$.

iii) The numerical error $\|u - u_j^\varepsilon\|_{H^s}$ for the approximate solution u_j^ε of (50) is less than $O(2^{-j(t-s)}\|u\|_{H^t})$ for $\mathbf{r} \le s \le t \le 2$, $s < \frac{3}{2}$, $\mathbf{r} + \frac{n}{2} < t$.

In Table 2 we compare the collocation method with the Galerkin method. We give the convergence orders, the regularity parameters γ, γ^*, $\tilde{\gamma}^*$, and the numbers of vanishing

moments d^*, $\tilde{d}^*$. These regularity parameters and vanishing moment conditions are required for the applicability of the discretization schemes (conformity), for the optimal compression rates, and for the preconditioning. Note that γ, γ^*, d^*, and d have been introduced in Section 3.1. The number $\tilde{\gamma}^*$ is the regularity parameter for the system $\{\tilde{\psi}_{l,k}\}$ dual to $\{\eta_{l,k}\}$, i.e., $\tilde{\psi}_{l,k} \in H^s$ for $s < \tilde{\gamma}^*$.

Galerkin:		
Regularity	$\gamma > \frac{\mathbf{r}}{2}$ for conformity	$\gamma^* > -\frac{\mathbf{r}}{2}$ for preconditioning
Van. Moments	$d^* > d - \mathbf{r}$	
Max. Conv. Rate		in $H^{\mathbf{r}-d}$: $2^{-j(2d-\mathbf{r})}$
Collocation:		
Regularity	$\gamma > \mathbf{r}$ for conformity	$\tilde{\gamma}^* > \frac{n}{2}$, $\gamma > \frac{n}{2} + \mathbf{r}$, $\tilde{\gamma}^* + \gamma^* > -\mathbf{r}$ for preconditioning
Van. Moments	$\tilde{d}^* > d - \mathbf{r}$	$d^* > -\mathbf{r}$
Max. Conv. Rate		in $H^{\mathbf{r}}$: $2^{-j(d-\mathbf{r})}$

Table 2: Comparison of Galerkin and collocation method.

For the boundary integral operator in Section 2.2, the assumptions of Theorem 6 are not satisfied. However, similarly to Theorem 6, we can prove that the compressed matrix A_j^ϵ defined with $a_0 = a_1 = a$, $\alpha = 5/6$, $\beta_1 = 2/3$, $\beta_2 = 4/3$, and $\beta_3 = 2/3$ contains no more than $O(N)$ times a power of $\log N$ non-zero entries. Moreover, the wavelet collocation including the compression is stable in L^2 and converges with order two. In Figure 5 we present the numerically obtained numbers of non-zero entries and compare these with the quadratic behaviour $O(N^2)$ for the fully populated matrices and with the linear behaviour $O(N)$. For a number $N = N_j = 4096$ and for the parameters $\bar{k} = 10$, $a = 0.3$, $\bar{k} = 10$, $a = 1.0$, and $\bar{k} = 1$, $a = 0.3$, respectively, the relative L^2 error of the single layer density function u is less than $3 \cdot 10^{-5}$, $3 \cdot 10^{-6}$, and $1 \cdot 10^{-7}$, respectively. Figure 6 shows the computation times for the iterative solution of the matrix equation with and without compression. The linear systems are solved by GMRes on a DEC 3000 AXP 500 α-processor workstation.

Now we turn to the boundary integral operator of Section 2.3 and consider the collocation method based on the bilinear splines of Section 3.2 together with the wavelet algorithm based on the wavelets from (25) and (47). Again, the assumptions of Theorem 6 are not satisfied. However, similarly to Theorem 6, we can prove that the compressed matrix A_j^ϵ defined with $a_0 = 1$, $a_1 = a$, $\alpha = 0$, $\beta_1 = 4/3$, $\beta_2 = 1$, and $\beta_3 = 1$ contains no more then $O(N^{4/3})$ entries. Moreover, the wavelet collocation including the compression is stable in L^2 and converges with order two. Though the compression is asymptotically not optimal, we believe that the presented choice of wavelets and compression parameters leads to faster computation times for $N \leq 10\,000$. In Table 3 we show the compression rates (compression rate = number N^2 of entries in the full matrix divided by the number of entries in the compressed matrix), the number of quadrature knots, and the computation times (including the time for the set up of the stiffness matrix). The time t_C and the number of knots k_C are given for the BEM without wavelets. The time t_D, the number

j	1	2	3	4	5
N_j	25	121	529	2209	9025
r_C	1	1	1	1	
k_C	$8 \cdot 10^3$	$1.25 \cdot 10^5$	$1.95 \cdot 10^6$	$3.1 \cdot 10^7$	
t_C	2.92s	6.64s	65.49s	1 005.81s	
r_D	1.19	2.69	6.83	12.64	13.99
k_D	$8 \cdot 10^3$	$1.0 \cdot 10^5$	$1.05 \cdot 10^6$	$1.07 \cdot 10^7$	$1.3 \cdot 10^8$
t_D	3.08s	6.06s	39.55s	405.17s	5 580.07s
r_P	1.19	2.69	6.83	19.44	36.90
k_P	$8 \cdot 10^3$	$1.0 \cdot 10^5$	$1.05 \cdot 10^6$	$9.4 \cdot 10^6$	$9.1 \cdot 10^7$
t_P	3.09s	6.06s	39.55s	351.63s	3 641.05s

Table 3: Compression rates, number of quadrature knots, and computation times.

of knots k_D, and the rate r_D correspond to the wavelet algorithm, where the compression parameter a is chosen such that the relative compression error for the unknown density u taken at four different points of $[0,1] \times [0,1]$ is less than 10^{-5}. For t_P, k_P, and r_P, the parameter a of the wavelet algorithm is chosen such that the relative compression error for a derivative of the single layer potential is less than 10^{-5}. The last error is taken over eight points in the exterior of the earth close to $\kappa(0.5, 0.5)$. Note that in the computation with the wavelet algorithms presented in Table 3 we solve the linear system (44) iteratively. The multiplication of a vector by A_j, however, is realized by applying the wavelet transform to the vector, by multiplying with the compressed and wavelet transformed matrix A_j^ε, and by applying the inverse wavelet transform.

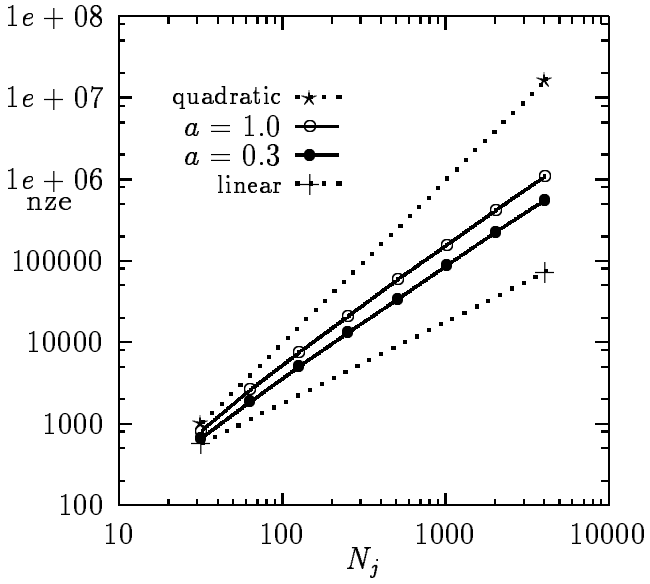

Figure 5: Number nze of nonzero elements of the compressed matrix for two constants a.

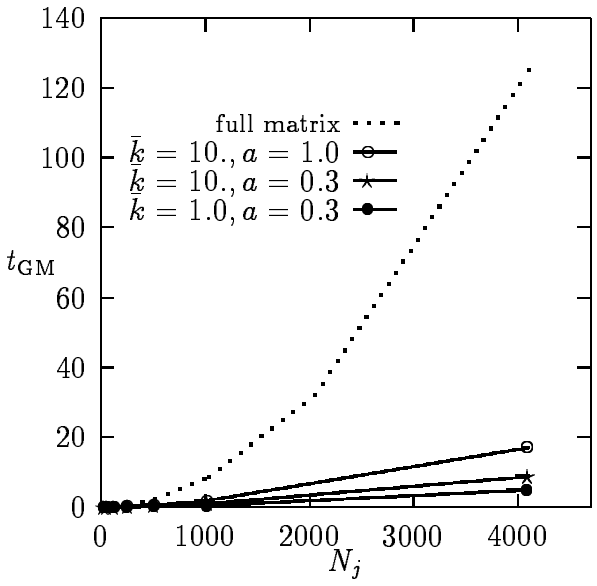

Figure 6: CPU-time t_{GM} in seconds for different wave numbers $\bar{k}$ and constants a.

5.4. THE ASSEMBLING OF THE MATRIX VIA QUADRATURE ALGORITHM

In order to concentrate on the essential issues of the matrix assembling we simplify formulae and notation. The conventional collocation algorithm is based on a stiffness matrix $(a_{x,\varphi})_{x,\varphi}$, where x runs through the set of collocation points and φ through the set of finite element basis functions. The entries take the form

$$\begin{aligned} a_{x,\varphi} &= (A\varphi)(x) = \int k(x,y)\varphi(y)\mathrm{d}y, \\ a_{x,\varphi} &\approx \sum_z k(x,z)\varphi(z)\omega_z, \end{aligned} \tag{51}$$

where $\int f \sim \sum_z f(z)\omega_z$ denotes a quadrature rule depending on the collocation point x. For the wavelet algorithm, the entries of the stiffness matrix $(a_{\eta,\psi})_{\eta,\psi}$ depend on the basis wavelet function ψ and on the test wavelet functional η. We get

$$\begin{aligned} a_{\eta,\psi} &= \eta(A\psi) = (A\psi)(x_1) - (A\psi)(x_2) \\ &= \int k(x_1,y)\psi(y)\mathrm{d}y - \int k(x_2,y)\psi(y)\mathrm{d}y\ , \\ a_{\eta,\psi} &\approx \sum_z k(x_1,z)\psi(z)\omega_z - \sum_z k(x_2,z)\psi(z)\omega_z\ , \end{aligned} \tag{52}$$

where, for simplicity, we consider wavelets like those in (47) for which $\eta(f) = f(x_1) - f(x_2)$ with certain x_1, x_2 depending on η. Now observe that the evaluation of the kernel functions costs much more time than the evaluation of the trial functions. Thus, the do loops of an efficient algorithm for the computation of (51) and (52) are to be arranged in such an order that the number of kernel evaluations is minimized. We, finally, arrive at the following algorithms for the conventional and the wavelet method, respectively:

do For all collocation points x.

Determine the quadrature rule with knots z and weights ω_z depending on x.

do For all quadrature knots z.

Compute $U = [k(x,z)\omega_z]$.

Determine all basis trial functions φ with $\varphi(z) \neq 0$.

do For all φ with $\varphi(z) \neq 0$.

Compute $T = U \cdot \varphi(z)$.

Add T to $a_{x,\varphi}$.

enddo

enddo

enddo

do For all collocation points x.

Determine all η s.t. $x \in \operatorname{supp}\eta$.

Determine the quadrature rule with knots z and weights ω_z depending on x.

do For all quadrature knots z.

Compute $U = [k(x,z)\omega_z]$.

Determine all basis trial functions ψ with $\psi(z) \neq 0$.

do For all ψ with $\psi(z) \neq 0$.

Compute $S = U \cdot \psi(z)$.

do For all η s.t. $x \in \operatorname{supp}\eta$.

Add $\pm S$ to $a_{\eta,\psi}$.

enddo

enddo

enddo

Comparing these algorithms, we observe that to the do loop over φ with $\varphi(z) \neq 0$ there corresponds the longer do loop over all ψ with $\psi(z) \neq 0$ and with $a_{\eta,\psi}$ not neglected in the compression step (though this is not indicated in the algorithm). To the addition of T to $a_{x,\varphi}$ there corresponds the do loop over all η such that $x \in \operatorname{supp}\eta$. We have chosen the wavelets in (25) and (47) so that the longer do loop over the ψ is not too long and that the additional do loop over the η is as short as possible. The wavelet algorithm can be faster than the conventional collocation only if the number of quadrature knots z in the corresponding do loop over z is less for the wavelet algorithm. Hence, the quadrature algorithm is essential. Before we turn to the quadrature algorithm we mention two important aspects. First, in order to reduce the time for input/output operations between CPU and main memory, we recommend to introduce an extra working field. For a fixed x, the entries $a_{\eta,\psi}$ with η such that $x \in \operatorname{supp}\eta$ and with arbitrary ψ should be stored in this two-dimensional field. Second, for the fast evaluation of the trial functions, the "tree" structure of the wavelet basis can be used. In fact, the values at a fixed point z for the wavelets and finite element functions of a certain level l can easily be obtained from the values for the functions of level $l+1$.

The quadrature algorithm for the assembling of the stiffness matrix A_j^ε should be based on the following (cf. [40]):

i) If the order $\mathbf{r}$ of A is non-negative, then the singular or hypersingular integrals in (52) should be regularized (cf. [30,45,34]) before quadrature rules are applied. E.g., for the singular kernel k of the boundary integral equation in (15), we split the kernel into the sum of a singular main part k_S and a weakly singular kernel. Then

j	accuracy 2^{-3j}	knots dyadic	max.knots per subinterval	knots equally spaced	max.knots per subinterval
3	$2 \cdot 10^{-3}$	8	2	16	2
5	$3 \cdot 10^{-5}$	24	3	96	3
7	$1 \cdot 10^{-6}$	48	4	384	3
10	$1 \cdot 10^{-9}$	108	6	4194	4
12	$2 \cdot 10^{-11}$	154	7	20864	5
14	$2 \cdot 10^{-13}$	208	8	-	-

Table 4: Quadrature errors and number of knots for the integral of a logarithmic function.

the integral in the integral operator takes the form

$$\int_{[0,1]\times[0,1]} k(x,y)u_h(y)\mathrm{d}y_1\mathrm{d}y_2 = u_h(x)\int k_S(x,y)\mathrm{d}y + \int [k(x,y)u_h(y) - k_S(x,y)u_h(x)]\,\mathrm{d}y. \tag{53}$$

Now the quadrature rules can be applied to the last integral which is weakly singular, only. The first integral on the right-hand side can be computed by an analytic formula.

ii) If the quadrature rule for the integral in $a_{\eta,\psi}$ is chosen in dependence not only on the collocation point $x \in \operatorname{supp}\eta$ but also on ψ (this means that a quadrature algorithm different from that presented above is used) and if the kernel is analytic, then composite Gauß rules over meshes graded geometrically towards the singularity point x can be applied. The order of the Gauß rule should increase slowly with decreasing distance to x. We have tested such a rule for $\int_0^{2\pi} \log(x-\pi)\mathrm{d}x$. In Table 4 we present the quadrature error, the number of knot points, and the maximal order of the Gauß rules. We compare a composite Gauß rule with variable Gauß order over the dyadic mesh $\{\pi \pm 2^{-l}\pi,\ l = 0,\ldots,j\}$ and a composite rule over the uniform partition $\{\pi \pm m \cdot 2^{1-j}\pi,\ m = 0,\ldots,2^{j-1}\}$ with a fixed order of the Gauß rule on each subinterval. Clearly, the rule over the graded mesh performs better. Note that in special cases quadrature rules with end point correction can also be applied (cf. [41,2]).

iii) The quadrature rule should be a composite tensor product Gauß rule and the underlying partition should be a refinement of the partition over which the trial functions are polynomials. More precisely, if the collocation point x is fixed, then we have to compute $\int k(x,y)\psi(y)\mathrm{d}y$ only for those ψ for which there is an η such that $x \in \operatorname{supp}\eta$ and such that $a_{\eta,\psi}$ is not discarded in the compression step. To this set of basis wavelets ψ there corresponds a minimal partition such that the ψ are polynomials on the subdomains. This partition is coarser than the partition of the level j, and we will call it starting partition. If we refine the starting partition over some subdomains near the singularity point x and take a composite Gauß rule, then we arrive at a suitable rule $\int f \sim \sum_z f(z)\omega_z$. Since the starting partition is coarser than the level j partition, the number of quadrature knots should be less than N^2.

iv) If the subdomain of the starting partition in iii) belongs to a level l coarser than level j, then no further partition step is needed. The order of the Gauß rule, which should be applied over the subdomain, can be fixed but should be greater or equal to the polynomial degree d of the trial functions plus the number of vanishing moments for the trial wavelets.

v) If the subdomain of the starting partition in iii) belongs to level j, then the quadrature technique for conventional collocation methods should be applied.

Note that the numbers of quadrature knots and the computation times (on a DEC 3000 AXP 400 α-processor workstation) presented in Table 3 are obtained with a quadrature algorithm based on i), iii)-v). The reduction in computation time is much less than the reduction in storage. This is due to the mesh grading over the subdomains of v). Using optimal rules for these subdomains, the reduction factor for the computation time should be similar to the compression rate.

REFERENCES

[1] ALPERT, B.K.: "A class of basis in L^2 for the sparse representation of integral operators", SIAM J. Math. Anal. 24, pp. 246–262, 1993.

[2] ALPERT, B.K.: "Rapidly-convergent quadratures for integral operators with singular kernels", Technical Report LBL 30092, Lawrence Berkeley Laboratory, University of California, Berkeley, CA, 1990.

[3] AMOSOV, B.A.: "On the approximate solution of elliptic pseudodifferential equations over smooth and closed curves", in Russian, Z. Anal. Anwendungen 9, pp. 545–563, 1990.

[4] ARNOLD, D.N. and WENDLAND, W.L: "The convergence of spline collocation for strongly elliptic equations on curves", Numer. Math. 47, pp. 317–431, 1985.

[5] BEYLKIN, G., COIFMAN, R., and ROKHLIN, V.: "Fast wavelet transforms and numerical algorithms I", Comm. Pure Appl. Math. 44, pp. 141–183, 1991.

[6] BRANDT, A. and LUBRECHT, A.A.: "Multilevel matrix multiplication and fast solution of integral equation", J. Comput. Phys. 90, pp. 348–370, 1991.

[7] CARNICER, J.M., DAHMEN, W., and PEÑA, J.M.: "Local decomposition of refinable spaces", to appear in Applied and Computational Harmonic Analysis, IGPM Report 112, RWTH Aachen, 1994.

[8] CHUI, C.K.: "An introduction to wavelets", Academic Press, Boston, 1992.

[9] COHEN, A., DAUBECHIES, I., and FEAUVEAU, J.-C.: "Biorthogonal bases of compactly supported wavelets", Comm. Pure and Appl. Math. 45, pp. 485–560, 1992.

[10] COLTON, D. and KRESS, R.: "Integral equation methods in scattering theory", Springer-Verlag, Berlin, Heidelberg, New York, 1983.

[11] DAHLKE, S., DAHMEN, W., HOCHMUTH, R., and SCHNEIDER, R.: "Stable multiscale bases and local error estimation for elliptic problems", IGPM Report 124, RWTH Aachen, 1996.

[12] DAHMEN, W., KLEEMANN, B., PROESSDORF, S., and SCHNEIDER, R.: "A multiscale method for the double layer potential equation on a polyhedron", in Dikshit, H.P. and Micchelli, C.A.: "Advances of Computational Mathematics", World Scientific Publ. Co., Inc., New Delhi, pp. 15–57, 1994.

[13] DAHMEN, W., KLEEMANN, B., PROESSDORF, S., and SCHNEIDER, R.: "Multiscale methods for the solution of the Helmholtz and Laplace equations", in Wendland, W.: "Boundary Element Methods", Reports from the Final Conference of the Priority Research Programme 1989-1995 of the German Research Foundation, Oct. 2-4, 1995, Stuttgart, Springer-Verlag, 1996.

[14] DAHMEN, W. and KUNOTH, A.: "Multilevel preconditioning", Numer. Math. 63, pp. 315–344, 1992.

[15] DAHMEN, W., KUNOTH, A., and SCHNEIDER, R.: "Operator equations, multiscale concepts and complexity", to appear in Proceedings of the AMS-SIAM Summer School, Park City, 1995, Preprint No. 206, WIAS, Berlin, 1996.

[16] DAHMEN, W., PROESSDORF, S., and SCHNEIDER, R.: "Multiscale methods for pseudo-differential equations", in Schumaker, L. and Webb, G.: "Recent Advances in Wavelet Analysis", Wavelet Analysis and its Application 3, pp. 191–235, 1994.

[17] DAHMEN, W., PROESSDORF, S., and SCHNEIDER, R.: "Wavelet approximation methods for pseudo-differential equations I: Stability and convergence", Math. Zeitschr. 215, pp. 583–620, 1994.

[18] DAHMEN, W., PROESSDORF, S., and SCHNEIDER, R.: "Wavelet approximation methods for pseudo-differential equations II: Matrix compression and fast solution", Advances in Comp. Math. 1, pp. 259-335, 1993.

[19] DAHMEN, W., PROESSDORF, S., and SCHNEIDER, R.: "Multiscale methods for pseudo-differential equations on smooth manifolds", in Chui, C.K., Montefusco, L., and Puccio, L.: "Wavelets: Theory, Algorithms, and Applications", Academic Press, pp. 1–40, 1994.

[20] DAUBECHIES, I.: "Ten lectures on wavelets", CBMS Lecture Notes 61, SIAM, Philadelphia, 1992.

[21] DOROBANTU, M.: "Potential integral equations of the 2D Laplace operator in wavelet basis", Preprint TRITA-NA-9401, Royal Institute of Technology, University of Stockholm, 1994.

[22] ENGELS, J. and KLEES, R.: "Galerkin versus collocation - Comparison of two discretization methods for the boundary integral equations in $\mathbb{R}^3$", Manuscripta Geodetica 17, pp. 245–256, 1992.

[23] GREENGARD, L. and ROKHLIN, V.: "A fast algorithm for particle simulation", J. Comput. Phys. 73, pp. 325–348, 1987.

[24] HACKBUSCH, W. and NOWAK, Z.P.: "On the fast matrix multiplication in the boundary element method by panel clustering", Numer. Math. 54, pp. 463–491, 1989.

[25] HARTEN, A. and YAD-SHALOM, I.: "Fast multiresolution algorithms for matrix-vector multiplication", SIAM J. Numer. Anal. 31, pp. 1191–1218, 1994.

[26] JUNKHERR, J.: "Effiziente Lösung von Gleichungssystemen die aus der Diskretisierung von schwach singulären Integralgleichungen 1. Art herrühren", Ph. D. Thesis, Christian-Albrechts-Universität Kiel, 1994.

[27] KLEES, R.: "Lösung des geodätischen Randwertproblems mit Hilfe der Randelementmethode", German Geodetic Kommission (DGK), Series C, No.382, Munich, 1992.

[28] MEYER, Y.: "Wavelets and Operators", Cambridge University Press, Cambridge, 1992.

[29] MIKHLIN, S.G. and PROESSDORF, S.: "Singular integral operators", Springer-Verlag, Berlin, Heidelberg, New York, Tokyo, 1986.

[30] NEDELEC, J.C.: "Integral equations with non integrable kernels", Integral Equations and Operator Theory 5, pp. 562–572, 1982.

[31] OSWALD, P.: "Multilevel finite element approximation", Teubner, Stuttgart, 1994.

[32] OVERHAUSER, A.W.: "Analytic definition of curves and surfaces by parabolic blending", Techn. Report No. S168-40, Scientific Research Staff Publication, Ford Motor Company, Detroit, 1968.

[33] PETERSDORFF, T.v. and SCHWAB, C.: "Boundary element methods with wavelets and mesh refinement", to appear in Proc. of ICIAM 1995, Hamburg, Special issue of ZAMM, Research Report No. 95-10, SAM, Eidgenössische Technische Hochschule Zürich, 1995.

[34] PETERSDORFF, T.v. and SCHWAB, C.: "Fully discrete multiscale Galerkin BEM", to appear in Dahmen, W., Kurdila, A.J., and Oswald, P.: "Multiresolution Analysis and PDE", Series: Wavelet Analysis and its Applications, Academic Press 1996, Research Report No. 95-08, SAM, Eidgenössische Technische Hochschule Zürich, 1995.

[35] PETERSDORFF, T.v. and SCHWAB, C.: "Wavelet approximations for first kind boundary integral equations on polygons", submitted to Numer. Math., Technical Note BN-1157, Institute for Physical Science and Technology, University of Maryland at College Park, 1994.

[36] PROESSDORF, S. and SCHMIDT, G.: "A finite element collocation method for singular integral equations", Math. Nachr. 100, pp. 33–60, 1981.

[37] PROESSDORF, S. and SCHNEIDER, R.: "A spline collocation method for multidimensional strongly elliptic pseudodifferential operators of order zero", Integral Equations and Operator Theory 14, pp. 399–435, 1991.

[38] PROESSDORF, S. and SCHNEIDER, R.: "Spline approximation methods for multidimensional periodic pseudodifferential equations", Integral Equations and Operator Theory 15, pp. 626–672, 1992.

[39] RATHSFELD, A.: "A wavelet algorithm for the solution of the double layer potential equation over polygonal boundaries", Journal of Integral Equations and Applications 7, pp. 47–97, 1995.

[40] RATHSFELD, A.: "A wavelet algorithm for the boundary element solution of a geodetic boundary value problem", Preprint No. 225, WIAS, Berlin, 1996.

[41] ROKHLIN, V.: "End point corrected trapezoidal quadrature rules for singular functions", Computers and Mathematics with Applications 20, pp. 52-61, 1990.

[42] ROKHLIN, V.: "Rapid solution of integral equations of classical potential theory", J. Comput. Phys. 60, pp. 187–207, 1983.

[43] SAAD, Y. and SCHULTZ, M.H.: "GMRES: A generalized minimal residual algorithm for solving nonsymmetric linear systems", SIAM J. Sci. Stat. Comput. 7, No.3, pp. 856–869, 1986.

[44] SARANEN, J. and VAINIKKO, G.: "Fast solvers of integral and pseudodifferential equations on closed curves", to appear.

[45] SAUTERS, S.: "Über die effiziente Verwendung des Galerkinverfahrens zur Lösung Fredholmscher Integralgleichungen", Ph. D. Thesis, Christian-Albrechts-Universität, Kiel, 1992.

[46] SAUTERS, S.: "Der Aufwand der Panel-Clustering-Methode für Integralgleichungen", Bericht Nr. 9115, Inst. f. Inform. u. Prakt. Math., Christian-Albrechts-Universität, Kiel, 1991.

[47] SCHNEIDER, R.: "Multiskalen- und Waveletkompression: Analysisbasierte Methoden zur effizienten Lösung großer vollbesetzter Gleichungssysteme", Habilitationsschrift, Fachbereich Mathematik, Technische Hochschule Darmstadt, 1995.

[48] STEPHAN, E.P. and TRAN, T.: "A multi-level additive Schwarz method for hypersingular integral equations", Report AMR94/24, University of New South Wales, Sydney, 1994.

[49] SWELDENS, W.: "The lifting scheme: a custom-design construction of biorthogonal wavelets", Technical Report, Industrial Mathematics Initiative, Department of Mathematics, University of South Carolina, 1994.

[50] WALKER, H.F.: "Implementation of the GMRES method using Householder transformations", SIAM J. Sci. Stat. Comput. 9, No. 1, pp. 152–163, 1988.